SERBIAN JOURNAL OF ELECTRICAL ENGINEERING
Vol. 12, No. 2, June 2015, 183-196

UDC: 621.311.24:681.5 **DOI: 10.2298/SJEE1502183M**

Series PID Pitch Controller of Large Wind Turbines Generator

Aleksandar D. Micić[1], Miroslav R. Mataušek[2]

Abstract: For this stable process with oscillatory dynamics, characterized with small damping ratio and dominant transport delay, design of the series PID pitch controller is based on the model obtained from the open-loop process step response, filtered with the second-order Butterworth filter F_{bw}. Performance of the series PID pitch controller, with the filter F_{bw}, is analyzed by simulations of the set-point and input/output disturbance responses, including simulations with a colored noise added to the control variable. Excellent performance/robustness tradeoff is obtained, compared to the recently proposed PI pitch controllers and to the modified internal model pitch controller, developed here, which has a natural mechanism to compensate effect of dominant transport delay.

Keywords: PID pitch control, Wind turbines generator, Oscillatory dynamics, Dominant dead-time, Modified internal model control.

1 Introduction

Recently, synthesis on PI-based pitch controller of large wind turbines generator is considered in [1, 2], where the process dynamics is defined by the following transfer function

$$G_p(s) = G_{p0}(s)\mathrm{e}^{-\tau s}, \quad G_{p0}(s) = \frac{a_2 s^2 + a_1 s + a_0}{s^4 + b_3 s^3 + b_2 s^2 + b_1 s + b_0}, \tag{1}$$

with parameters in **Table 1** [1], for two processes denoted as $G_{p1}(s)$ and $G_{p2}(s)$.

It is supposed in [1, 2] that hydraulic pitch actuator AC is applied, modeled as a dead-time τ. Thus, process is defined by $\mathrm{AC} = \exp(-\tau s)$ in series with $G_{p0}(s)$, as in (1). Transfer function (1) defines a single-input single-output process, where input is the blade pitch angle and output defines tower fore-aft deflection. Processes $G_{pi}(s)$, i = 1, 2, exhibit a strong resonant response even by the small amount of excitation which is naturally present in the wind [3].

[1]Faculty of Technical Sciences, University of Priština, Kosovska Mitrovica, Kneza Miloša 7, Serbia;
E-mail: admicic@gmail.com
[2]School of Electrical Engineering, University of Belgrade, Kralja Aleksandra 73, Belgrade, Serbia;
E-mail: matausek@etf.rs

Table 1
Parameters of $G_{p1}(s)$ and $G_{p2}(s)$.

Process	a_2	a_1	a_0	b_3	b_2	b_1	b_0	τ
$G_{p1}(s)$	−0.6219	−8.7165	−2911	5.018	691.3	1949	$1.15 \cdot 10^5$	0.25
$G_{p2}(s)$	2.426	−4.6345	−147.3	4.857	126.2	266.4	$3.66 \cdot 10^3$	0.25

Design of pitch controllers based on the process dynamics characterization (1), as in [1, 2], is a complex control problem: to design a controller with a good performance/robustness tradeoff for the process with oscillatory dynamics, characterized with small damping ratio and dominant transport delay. Investigation presented in [4] is performed to demonstrate how to apply optimization to tune parallel PID controller for process (1) with strong resonant response.

In the present paper design of pitch controllers is based on the methods proposed for series PID controller in [5] and for Modified Internal Model Control (MIMC) in [6]. In Section 2, control relevant models $G_{\text{pid}}(s)$, and $G_{\text{mimc2}}(s)$, of processes $G_{p1}(s)$ and $G_{p2}(s)$, are determined by applying a simple procedure. In Section 3, design of PID and MIMC pitch controllers are performed based on models determined in Section 2. As demonstrated in Section 3, MIMC controller has a natural mechanism to compensate effect of dominant dead-time. This is the reason why the MIMC pitch controller, providing excellent performance/robustness tradeoff, is also used to demonstrate properties of the proposed series PID pitch controller. In Section 4, closed-loop simulation results are presented and compared with results obtained by PI controllers from [1, 2]. Simulations with a colored noise added to the control variable are also presented and used to simulate effect of the stochastic wind variation on the tower fore-aft deflection. Finally, simulations with strong rate constraints in actuator are used to demonstrate advantages of the series PID pitch controller and PI pitch controller proposed here.

2 Models Used in the Proposed Pitch Controller Design

Control relevant models $G_{\text{mimc2}}(s)$, used for the MIMC pitch controller design, are defined by

$$G_{\text{mimc}}(s) = G_{\text{mimc0}}(s)\,\mathrm{e}^{-\tau_{\text{mimc}}s}, \quad G_{\text{mimc0}}(s) = K\frac{T_z s + 1}{T^2 s + 2\xi T s + 1} \tag{2}$$

and **Table 2**. Simple process dynamics characterization is used to obtain control relevant models (2) by applying fitting-by-eye technique to approximate open-loop step responses of stable processes $G_{p1}(s)$ and $G_{p2}(s)$.

Table 2
Parameters of models (2) *used in the MIMC pitch controller design.*

Process/Model	K	T	T_z	ξ	τ_{mimc}
$G_{p1}(s)/G_{mimc1}(s)$	−0.0253	0.05	0.10	0.018	0.42
$G_{p2}(s)/G_{mimc2}(s)$	−0.0402	0.14	0.42	0.060	0.51

Responses of model (2), compared to responses of process $G_p(s)$ in (1), are presented in Fig. 1. From Fig. 1, and **Table 2**, it follows that the oscillatory dynamics of processes $G_{p1}(s)$ and $G_{p2}(s)$ is characterized by small damping ratio ξ and dominant dead-time τ_{mimc}, larger than time constant T. The nonminimum-phase characteristics of $G_{p2}(s)$ response are included in the dead-time of model $G_{mimc2}(s)$, as demonstrated in Fig.1b. Similar values of the time constant T=0.1398 and damping ratio $\xi = 0.0618$, as in the second raw of **Table 2**, are obtained from the dominant complex-conjugate pole pair of $G_{p2}(s)$, at s_1= −0.4416 +7.1373i and s_2= −0.4416 −7.1373i.

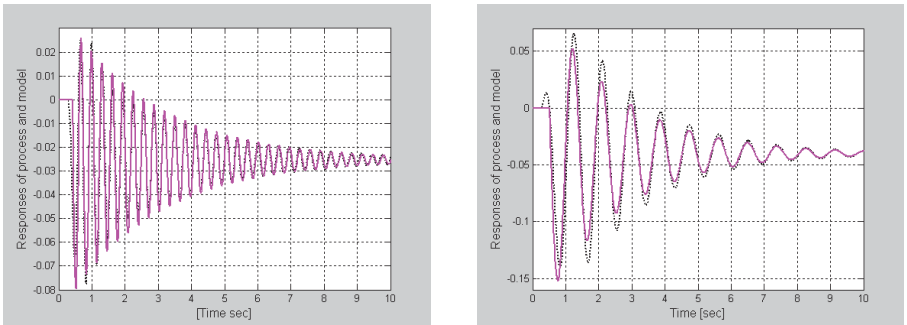

(a) (b)

Fig. 1 – *Unit step response of $G_{pj}(s)$, j = 1, 2, (dotted) and models $G_{mimc,j}(s)$ (solid):* a) $G_{p1}(s)$ *and* $G_{mimc1}(s)$, b) $G_{p2}(s)$ *and* $G_{mimc2}(s)$.

Control relevant models $G_{pid}(s)$ are obtained by applying fitting-by-eye technique to approximate filtered open-loop step responses $G_p(s)F_{bw}(s)$ of stable processes $G_{p1}(s)$ and $G_{p2}(s)$, with oscillatory dynamics, as proposed in [5]. The second-order Butterworth filter $F_{bw}(s)$ is used here in the form

$$F_{bw}(s) = \frac{1}{T_{fb}^2 s^2 + \sqrt{2}T_{fb}s + 1}. \tag{3}$$

Models $G_{pid}(s)$ are defined by **Table 3** and

$$G_{\text{pid}}(s) = G_{\text{pid}0}(s)e^{-\tau_{\text{pid}}},\ G_{\text{pid}0}(s) = K/[(T_1 s+1)(T_2 s+1)],\quad T_1 = T_2\,. \tag{4}$$

Table 3

Parameters of models (4) *used in the series PID pitch controller design.*

Process/Model	T_{fb}	K	T_1	T_2	τ_{pid}
$G_{p1}(s)/G_{\text{pid1}}(s)$	1.00	−0.0253	0.72	0.72	0.5
$G_{p2}(s)/G_{\text{pid2}}(s)$	1.41	−0.0402	1.00	1.00	0.6
$G_{p2}(s)/G_{\text{pid2,2}}(s)$	2.00	−0.0402	1.50	1.50	0.6

Process responses and filtered responses $G_p(s)F_{bw}(s)$, with $F_{bw}(s)$ from (3) and **Table 3**, are compared in Figs. 2 and 3 to responses of models $G_{\text{pid}}(s)$ from (4) and **Table 3**. Correct values of parameters for model $G_{\text{pid1}}(s)$, denoted in [4] as $G_{\text{SO1}}(s)$, are presented in **Table 3**.

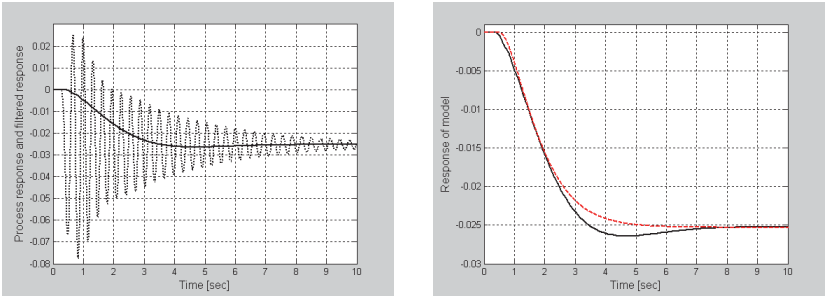

(a) (b)

Fig. 2 – *Determination of model used to design series PID$_1$ controller: a) unit step response of $G_{p1}(s)$ (dotted) and filtered response $G_{p1}(s)F_{bw}(s)$ with T_{fb} = 1 (solid),* b) *filtered response (solid) and model response $G_{\text{pid1}}(s)$ (dashed).*

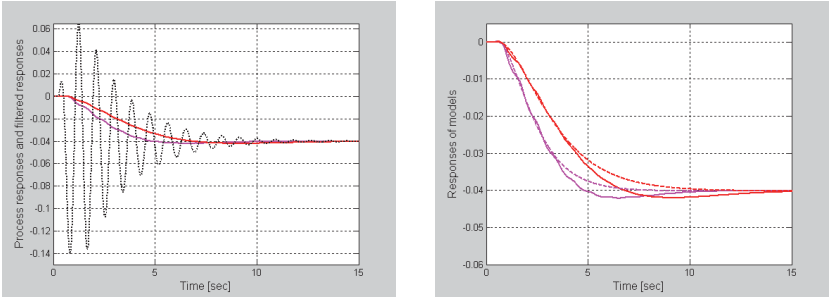

(a) (b)

Fig. 3 – *Determination of models used to design series PID$_2$ controllers:* a) *unit step response of $G_{\text{p2}}(s)$ (dotted) and filtered responses $G_{p2}(s)F_{\text{bw}}(s)$ with T_{fb} = 1.41 (solid-magenta) and T_{fb} = 2 (solid-red),* b) *filtered responses and model responses $G_{\text{pid2,1}}(s)$ (dashed-magenta) and $G_{\text{pid2,2}}(s)$ (dashed-red).(Colors can be seen in electronic version),*

3 Control System Design and Tuning

Structure of the MIMC pitch controller is presented in Fig. 4. Transfer function $G_{\text{mimc}0}^{-1}(z) = K^{-1}W_z(z)W_p(z)$ is a discrete inverse of the model $G_{\text{mimc}0}(s)$ [6], defined by parameters in **Table 2** and adopted sampling period Δt. By applying a discretization procedure [6], from (2) one obtains

$$W_p(z) = \frac{z^2 + a_{p1}z + a_{p2}}{(1 + a_{p1} + a_{p2})z^2}, a_{p2} = \exp(-2\xi\Delta t / T), \tag{5}$$

$$a_{p1} = -2\exp(-\xi\Delta t / T)\cos\left(\frac{\Delta t}{T}\sqrt{1-\xi^2}\right), \tag{6}$$

while

$$W_z(z) = (1-b)z/(z-b), \quad b = \exp(-\Delta t / T_z).$$

Transfer function $G_L(z) = z^{-(L+1)}$, where $L \approx \tau_{\text{mimc}}/\Delta t$. Filter $F(z)$ in Fig. 4, for $F_r(z) \equiv 1$ defines the desired closed-loop system time constant T_{CL} [6]. In the present paper $F(z)$ is designed as a discrete equivalent of the second-order low-pass filter $1/(T_C s + 1)^2$

$$F(z) = \left(\frac{(1-\alpha)z}{z-\alpha}\right)^2, \quad \alpha = \exp(-\Delta t / T_c), T_c = 0.4. \tag{7}$$

Tuning parameters T_{C}, and α in (7), are defined by the desired value of the time constant T_{CL}, for the second-order filter equal to $T_{\text{CL}} \approx 2T_{\text{C}}$. The adopted value of $T_{\text{C}} = 0.4$ s corresponds to the closed-loop system time constant obtained with PI controllers from [1, 2]. Since $T_{\text{CL}} \approx 0.8$ s, the sampling period $\Delta t = 0.05$ s is used to define filter $F(z)$ in (7), with $\alpha = 0.8825$, and to design MIMC$_j$, j = 1, 2 controllers.

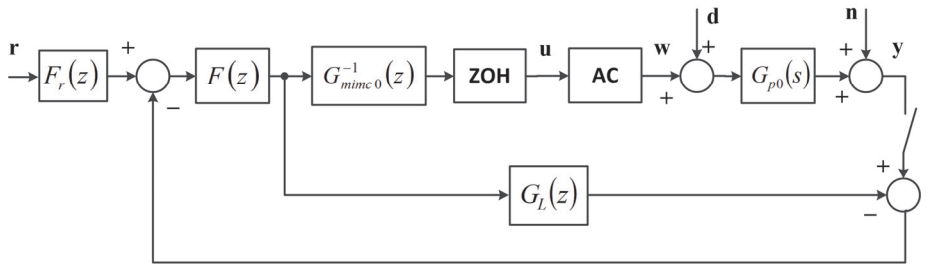

Fig. 4 – *MIMC pitch control system structure with set-point prefilter $F_r(z)$, Zero-Order Hold (ZOH) and actuator AC. Input and output disturbances are denoted by d and n.*

Thus, for $G_{p1}(s)$, from $G_{\text{mimc1}}(s)$ and $\Delta t = 0.05$ s, one obtains in the MIMC$_1$ controller $G_{\text{mimc0}}^{-1}(z) = K^{-1}W_z(z)W_p(z)$,

$$G_{\text{mimc0}}^{-1}(z) = (-0.0253)^{-1}\frac{(1-0.606)z}{z-0.606}\frac{z^2-1.0616z+0.9646}{(1-1.0616+0.9646)z^2}, \tag{8}$$

$$G_L(z) = z^{-9}, \tag{9}$$

while for $G_{p2}(s)$, from $G_{\text{mimc2}}(s)$ and $\Delta t = 0.05$ s, one obtains in the MIMC$_2$ controller

$$G_{\text{mimc0}}^{-1}(z) = (-0.0402)^{-1}\frac{(1-0.8878)z}{z-0.8878}\frac{z^2-1.8345z+0.9580}{(1-1.8345+0.9580)z^2}, \tag{10}$$

$$G_L(z) = z^{-11}. \tag{11}$$

MIMC controllers are defined by Fig. 4 where $F(z)$, $G_{\text{mimc0}}^{-1}(z)$ and $G_L(z) = z^{-(L+1)}$ are defined by (7) – (11). The same filter $F(z)$ in (7) with $\alpha = 0.8825$ is used in both MIMC$_j$, $j = 1, 2$ controllers, implemented with sampling period $\Delta t = 0.05$ s.

Anti-Reset Windup (ARW) implementation from [5], presented in Fig. 5, is used for the PID pitch controller with parameters K_p, T_i, T_d, T_{fb} defined in **Table 4**. To obtain satisfactory set-point following response this implementation requires a set-point prefilter $F_r(s) = F_{bw}(s)$.

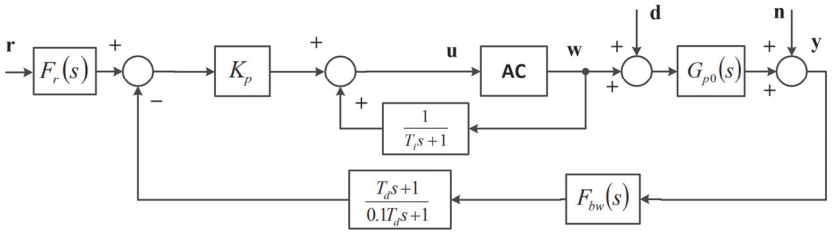

Fig. 5 –*Anti-reset windup implementation of the series PID pitch controller. For AC =* exp(–τ*s*) *one obtains linear case, without amplitude or rate constraints in actuator AC. Set-point prefilter* $F_r(s) = F_{bw}(s)$.

Parameters of the series PID pitch controller in Fig. 5 are given in **Table 4**. They are obtained by applying models $G_{\text{pid}}(s)$ defined by (4), **Table 3** and Simple Control (SIMC) tuning rules from [7] used to determine proportional gain, integral time T_i and derivative time T_d as proposed in [7]. According to **Table 3**, it is used $T_1 = T_2$ in (12). Besides the Butterworth filter F_{bw}, series PID pitch controller includes a low-pass filter $1/(T_f s+1)$ in the term defining derivative action $(T_d s+1)/(T_f s+1)$, where $T_f = T_d/10$.

$$K_p = \frac{T_1}{2K\tau_{\text{pid}}}, \quad T_2 \le T_1, \quad T_i = \min\{T_1, 8\tau_{\text{pid}}\}, \quad T_d = T_2. \tag{12}$$

Table 4
Parameters of series PID pitch controllers.

Controller/Process	K_p	T_i	T_d	T_{fb}
$\text{PID}_1/G_{p1}(s)$	−28.46	0.72	0.72	1.00
$\text{PID}_{2,1}/G_{p2}(s)$	−20.73	1.00	1.00	1.41
$\text{PID}_{2,2}/G_{p2}(s)$	−31.09	1.50	1.50	2.00

According to results in **Table 4**, series PID pitch controllers can be implemented also as digital controllers by using sampling period $\Delta t = 0.05$ s. However, they are implemented as continuous controllers, defined by Fig. 5, and parameters in **Table 4**. Continuous PI pitch controllers from [1, 2] are implemented as continuous controllers, in a standard way, with proportional and integral gains K_p and K_i defined by **Table 5.**

Table 5
Parameters of PI pitch controllers from [1, 2].

Controller/process	K_p	K_i
$\text{PI}_1/G_{\text{p1}}(s)$	1.0242	−20.5914
$\text{PI}_2/G_{\text{p2}}(s)$	1.0000	−20.0000

4 Results of Closed-Loop Simulation

As in [1, 2] in linear case, actuator is modeled as the dead-time, $\text{AC} = \exp(-0.25s)$. Anti-Reset Windup (ARW) implementation from [5] presented in Fig. 5, is used for the PID pitch controller, with parameters K_p, T_i, T_d, T_{fb} in **Table 4**.

Closed-loop system responses obtained by the PID pitch controllers are compared in Figs. 6 – 9 with results obtained by the MIMC pitch controller with $F_r(z) \equiv 1$, and obtained by PI pitch controllers from [1, 2] defined by **Table 5**. Parameters of the PI_1 controller are obtained in [2] by unconstrained minimization of IAE_r, the integrated absolute error following the unit step set-point response. Parameters of the PI_2 controller are taken from the stabilizing region in the $K_i - K_p$ plane [1, Fig. 2, for $K_i < 0$], as a good compromise between performance and robustness.

The desired closed-loop system time constant equal to $2T_C = 0.8$ s, is satisfied almost exactly by applying MIMC controllers. For better performance, demonstrated in Fig. 6a, and similar performance in Fig. 7a, better robustness is obtained by the PID and MIMC controllers, as demonstrated by the robustness indices in **Table 6**, where performance/robustness tradeoff obtained by PI, PID and MIMC controllers is presented.

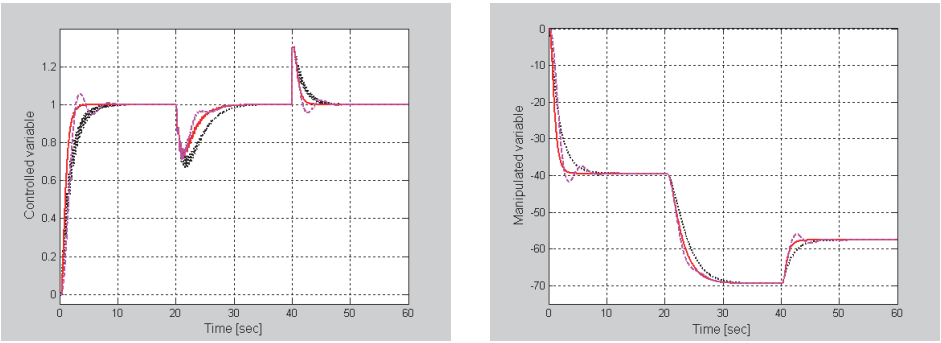

(a) (b)

Fig. 6 – *Closed-loop system responses of nominal process $G_{p1}(s)$, with controllers: $MIMC_1$ (solid), PID_1 (dashed) and PI_1 (dotted). Input and output disturbances: $D(s) = 30\exp(-20s)/((2s+1)s)$ and $N(s) = 0.3\exp(-40s)/s$.*

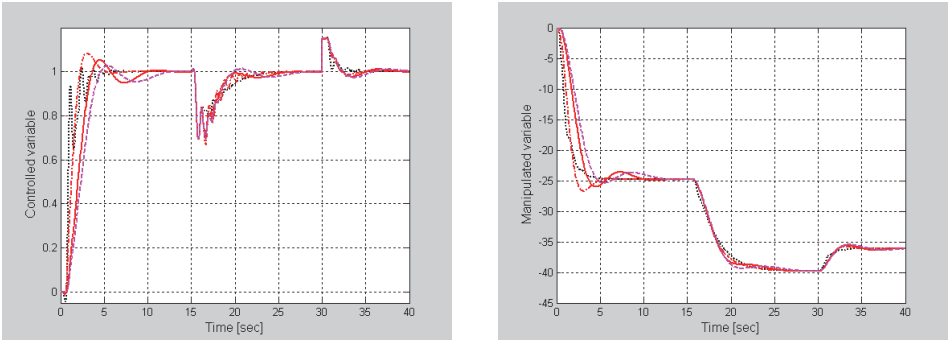

(a) (b)

Fig. 7 – *Closed-loop system responses of nominal process $G_{p2}(s)$ with controllers: $MIMC_2$ (dash-dot), $PID_{2,1}$ (solid), $PID_{2,2}$ (dashed) and PI_2 (dotted). Input and output disturbances: $D(s) = 15\exp(-15s)/((2s+1)s)$ and $N(s) = 0.15\exp(-30s)/s$.*

Performance index IAE_n, in **Table 6**, is the integrated absolute error following the unit step output disturbance $N(s) = 1/s$, obtained in simulation with the input disturbance $D(s) = 0$ and set-point $R(s) = 0$.

Variances in **Table 6**, are calculated as

$$\sigma_y^2 = \int_0^{T_{sim}} y^2(t)\,\mathrm{d}t / T_{sim}\ , \tag{13}$$

where T_{sim} is the simulation time interval $T_{sim} = 60$ s and $y(t)$ is the controlled variable response. Simulation is performed with the input disturbance $D(s) = 0$, set-point $R(s) = 0$ and output disturbance $n(t)$ defined by a Band-Limited White Noise (BLWN) $n(t)=n_w(t)$. It is obtained from a BLWN generator with power $b_w = 0.0005$ and sample time $T_s = \Delta t = 0.05$s. The variance of this BLWN $n_w(t)$ is theoretically equal to $b_w/T_s = 0.01$ [8, Appendix A]. Thus, as demonstrated in **Table 6**, all controllers guarantee low value of variance σ_y^2.

Table 6

Performance/robustness tradeoff obtained with PI, MIMC and PID controllers.

Controller/Process	IAE_n	σ_y^2	M_S	M_T
$PI_1/G_{p1}(s)$	1.93	0.01139	4.01	3.06
$MIMC_1/\ G_{p1}(s)$	1.17	0.01037	1.38	1.00
$PID_1/\ G_{p1}(s)$	1.42	0.01056	1.62	1.20
$PI_2/G_{p2}(s)$	1.26	0.01147	2.17	1.40
$MIMC_2/\ G_{p2}(s)$	1.49	0.01043	1.54	1.01
$PID_{2,1}/\ G_{p2}(s)$	1.81	0.01060	1.62	1.25
$PID_{2,2}/\ G_{p2}(s)$	1.96	0.01055	1.54	1.28

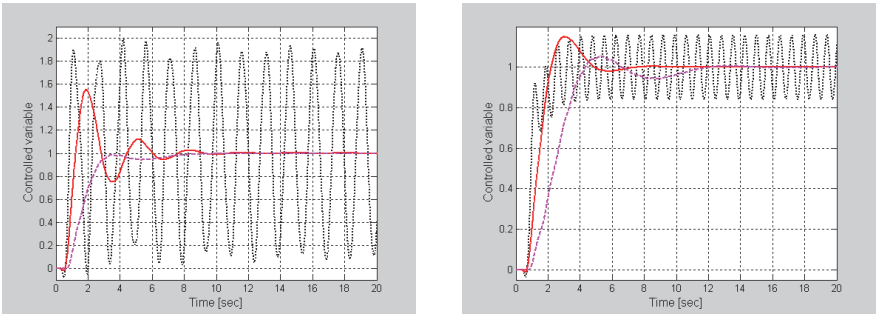

(a) (b)

Fig. 8 – *Closed-loop system set-point responses of perturbed process $G_{p2}(s)$, with controllers: $PID_{2,2}$ (dashed), $MIMC_2$ (solid) and PI_2 (dotted). In* a) *perturbed gain, $G_{p2\text{pert}}(s) = 2.04G_{p2}(s)$,* b) *perturbed dead-time, greater* 44%, $G_{p2\text{pert}}(s) = G_{p2}(s)\exp(-0.11s)$.

It is important that performance/robustness tradeoff obtained by the series PID pitch controller depends weakly on the choice of the time constant T_{fb}. This is demonstrated in Figs. 7a and 7b and confirmed in **Table 6**, for two values T_{fb}=1.41 and T_{fb}=2, resulting into practically equal performance/robustness tradeoff for evidently different model responses in Fig. 3b.

Excellent responses are obtained for the perturbed process $G_{p2}(s)$, with the proposed $PID_{2,2}$ pitch controller compared in Fig. 8 to $MIMC_2$ dead-time compensating pitch controller and PI_2 pitch controller. High values of robustness indices M_S and M_T in **Table 6**, obtained by the PI_1 controller, are consequence of unconstrained optimization applied in [2].

Robustness indices, maximum sensitivity M_S and maximum complementary sensitivity M_T, are defined by the sensitivity function $S(s) = 1/(1+L(s))$ and complementary sensitivity $T(s) = 1-S(s)$ as

$$M_S = \max_\omega \left|S(i\omega)\right|, \quad M_T = \max_\omega \left|T(i\omega)\right|. \tag{14}$$

Loop transfer function is defined by $L(s) = G_{p0}(s)C(s)$. From Fig. 4 and AC= $\exp(-\tau s)$, one obtains that $C(s)$, in $L(s) = G_{p0}(s)C(s)$, used to obtain robustness indices M_S and M_T for MIMC controllers, is given by

$$C(s) = \mathrm{e}^{-\tau s}\, G_{mimc0}^{-1}(z)F(z) / (1 - F(z)G_L(z))\Big|_{z=\exp(s\Delta t)}. \tag{15}$$

For the series PID controllers, from Fig. 5 and AC= $\exp(-\tau s)$, one obtains $C(s)$ given by

$$C(s) = K_p \frac{T_i s + 1}{T_i s} \mathrm{e}^{-\tau s} \frac{T_d s + 1}{0.1 T_d s + 1} F_{bw}(s), \tag{16}$$

in $L(s) = G_{p0}(s)C(s)$. For PI controllers, PI_1 from [2] and PI_2 from [1], one obtains.

$$C(s) = \left(K_p + \frac{K_i}{s} \right) \mathrm{e}^{-\tau s}. \tag{17}$$

Finally, to illustrate influence of wind speed variation on the tower fore-aft deflection, simulation is performed with the set-point $R(s)$=0 ,output disturbance $N(s)$=0 and with noise $n_{\mathrm{wind}}(t)$ acting as an unknown input disturbance $d(t) = n_{\mathrm{wind}}(t)$. Stochastic variation of the wind speed $n_{\mathrm{wind}}(t)$ is obtained from a BLWN generator with power $b_w = 0.0001$ and sample time $T_s = 0.01$ s, passed through the low-pass filter $F(s) = 1/(5s + 1)$. Results of this simulation are summarized in Fig. 9 and **Table 7**. Variances presented in **Table 7** are calculated as in (13) for the simulation time interval $T_{\mathrm{sim}} = 60$ s.

Random variation of the simulated wind speed acts on the blade pitch angle as presented in Fig. 9a. As a result the tower fore-aft deflection is obtained as in Fig. 9b. Smaller variation of the tower fore-aft deflection is obtained by the MIMC and PID controllers, with significantly smaller control signal activity, moves up and down of the manipulated variable $w(t)$, demonstrated in Fig. 9a.

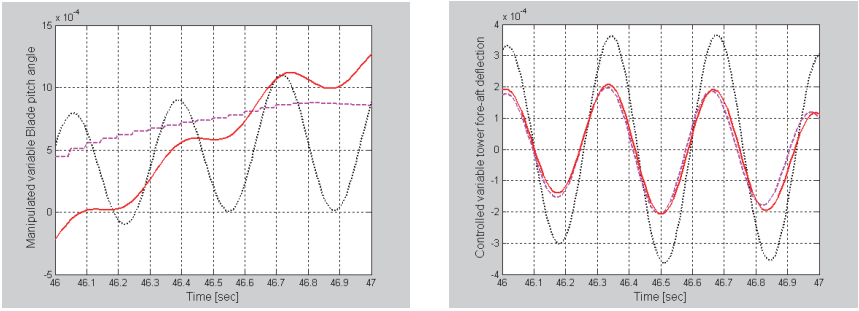

(a) (b)

Fig. 9 – *A part of closed-loop system responses of nominal process $G_{p1}(s)$ with controllers: PI_1 (dotted), PID_1 (solid) and $MIMC_1$ (dashed). Only input disturbance is active, simulating stochastic variation of the wind speed.*

Table 7

Variances obtained with PI, PID and MIMC controllers.

Controller/Process	σ_y^2
$PI_1/G_{p1}(s)$	22.23e-09
$PID_1/G_{p1}(s)$	9.69e-09
$MIMC_1/G_{p1}(s)$	8.46e-09

For almost the same response of the tower fore-aft deflection in Fig. 9b, much better reduction of the control signal activity is obtained by the MIMC controller in Fig. 9a.

However, analyses presented until now were performed for the linear case, for the actuator $AC= \exp(-\tau s)$. In industrial applications constraints in actuators are inevitable. In this case advantage of the proposed PID controller in Fig. 5 is its antiwindup structure.

To illustrate performance of PI, PID and MIMC controllers in the presence of rate constraints in actuator, results of simulation with and without rate constraints are compared in Fig. 10, for process $G_{p1}(s)$ with controllers: PI_1 PID_1 and $MIMC_1$.

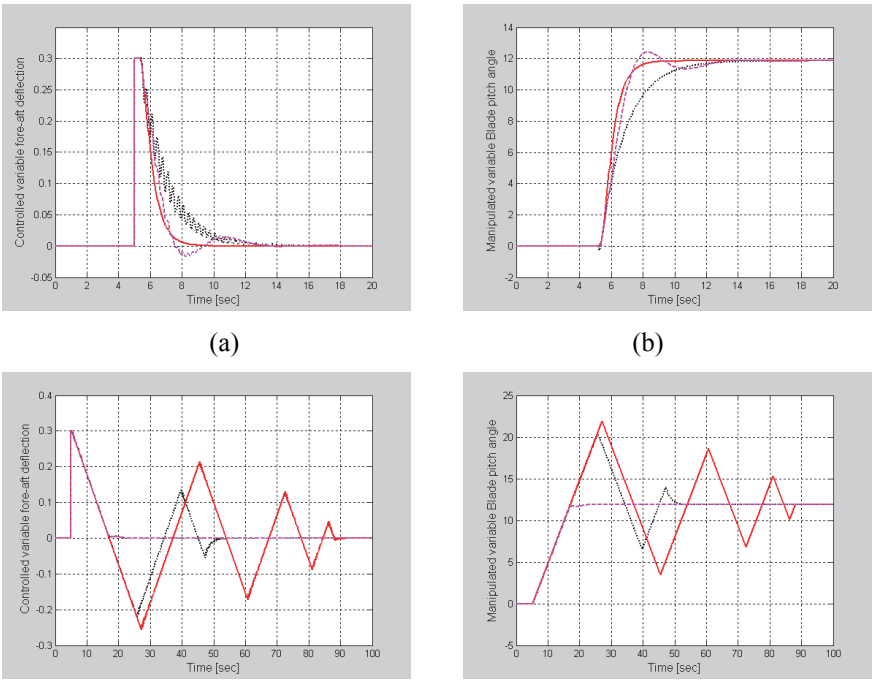

Fig. 10 – *Closed-loop system responses of nominal process* $G_{p1}(s)$ *with controllers:* PI_1 *(dotted),* $MIMC_1$ *(solid) and* PID_1 *(dashed) for* $R(s) = 0$, $D(s) = 0$ *and* $N(s) = 0.3\exp(-5s)/s$. *In* a) – b) *without rate constraints and in* c) – d) *with strong rate constraints: rising rate* $1s^{-1}$ *and falling rate* $-1s^{-1}$.

Finally, results of simulation with and without rate constraints are compared in Fig. 11, for process $G_{p1}(s)$ with controllers: $\mathrm{PID_1}$ and $\mathrm{PI_{1new}}$. Controller $\mathrm{PI_{1new}}$ is proposed here. It is obtained by applying SIMC rules to simplify the Second-Order Plus Dead-Time (SOPDT) model $G_{\mathrm{pid1}}(s)$ to the First-Order Plus Dead-Time (FOPDT) model $G_{\mathrm{pi1}}(s)$, given by

$$G_{\mathrm{pi1}}(s) = \frac{K\,\mathrm{e}^{-\tau s}}{(Ts+1)}, \quad T = T_1 + T_2/2, \quad \tau = \tau_{\mathrm{pid}} + T_2/2\,, \tag{18}$$

where parameters K, $T_1{=}T_2$ and τ_{pid} are taken from the first row in Table 3.

$\mathrm{PI_{1new}}$ controller is implemented as in Fig. 5, with $T_d{=}0$, time constant T_{fb} from the first row of **Table 3**, K_p and T_i T_{i} defined by (18) and tuning rule [7]

$$K_p = \frac{T}{2K\tau}, \quad T_i = \min\{T, 8\tau\}\,. \tag{19}$$

Results in Fig. 11 confirm that an effective anti-reset windup PI pitch controller for process $G_{p1}(s)$ can be easily obtained by the procedure proposed here.

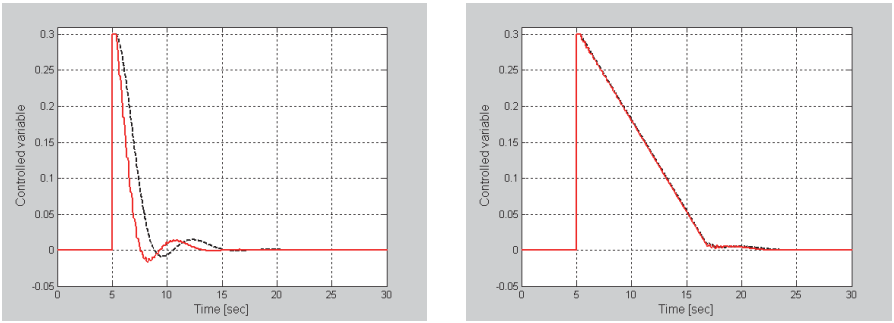

(a) (b)

Fig. 11 – *Closed-loop system responses of nominal process $G_{p1}(s)$ with controllers: PID_1 (solid) and PI_{1new} (dashed), for $R(s)$, $D(s)$ and $N(s)$ as in Fig. 10. In* a) *without rate constraints. In* b) *with strong rate constraints as in Fig. 10.*

Due to space limitations, further analyses with the PI pitch controller proposed here is not presented. However, presented details makes possible to repeat some previous simulations with the PI_{1new} controller, as well as to design a PI_{2new} controller for process $G_{p2}(s)$. It is believed that design of PI/PID pitch controller proposed here is important for further development and comparative analyses of pitch controllers.

5 Conclusion

Better performance/robustness tradeoff is obtained with the MIMC and PID pitch controller, compared to PI pitch controllers from [1, 2].

It is important that inclusion of derivative action, in the presence of the simulated stochastic variation of the wind, results into performance improvement obtained with the reduced control signal activity. Better reduction of the control signal activity is obtained with the proposed MIMC controller. However, advantage of the proposed PID controller in Fig. 5 is its antiwindup structure.

Tuning of the proposed PID and PI pitch controller is simple and can be performed experimentally, by applying SIMC tuning rules to SOPDT model $G_{\text{pid}}(s)$ and FOPDT model $G_{\text{pi}}(s)$, both determined from open-loop process step responses memorized for different operating regimes.

6 Acknowledgement

A.D. Micić acknowledges financial support from the Serbian Ministry of Science and Technology (Project III 47016).

7 References

[1] J. Wang, N. Tse, Z. Gao: Synthesis on PI-based Pitch Controller of Large Wind Turbines Generator, Energy Conversion and Management, Vol, 52, No. 2, Feb. 2011, pp. 1288 – 1294.

[2] J.W. Perng, G.Y. Chen, S.C. Hsieh: Optimal PID Controller Design based on PSO-RBFNN for Wind Turbine Systems, Energies, Vol. 7, No. 1, Jan. 2014, pp. 191 – 209.

[3] E.A. Bossanyi: The Design of Closed-loop Controllers for Wind Turbines, Wind Energy, Vol. 3, No. 3, July/Sept.2000, pp. 149 – 163.

[4] T.B. Šekara, M.R. Mataušek: Design of PI/PID controller for control of blades angle of high power wind turbine, ETRAN Conference, Vrnjačka Banja, Serbia, 02-05 June 2014, p. AU2.1.1-3. (In Serbian).

[5] M.R. Mataušek, B.T. Jevtović, I.M. Jovanov: Series PID Controller Tuning based on the SIMC Rule and Signal Filtering, Journal of Process Control, Vol. 24, N. 5, May 2014, pp. 687 – 693.

[6] M.R. Mataušek, A.D. Micić, D.B. Dačić: Modified Internal Model Control Approach to the Design and Tuning of Linear Digital Controllers, International Journal of Systems Science, Vol. 33, No. 1, 2002, pp. 67 – 79.

[7] S. Skogestad: Simple Analytic Rules for Model Reduction and PID Controller Tuning, Journal of Process Control, Vol 13, No 4, June 2003, pp. 291 – 309.

[8] A.D. Micić, M.R. Mataušek: Optimization of PID controller with Higher-order Noise Filter, Journal of Process Control, Vol. 24, No. 5, May 2014, pp. 694 – 700.